OXFORD

Briefings in Bioinformatics, 2022, **23**(3), 1–15
https://doi.org/10.1093/bib/bbac047
Problem Solving Protocol

Systematic optimization of host-directed therapeutic targets and preclinical validation of repositioned antiviral drugs

Dafei Xie†, Song He†, Lu Han†, Lianlian Wu, Hai Huang, Huan Tao, Pingkun Zhou, Xunlong Shi, Hui Bai and Xiaochen Bo

Corresponding authors: Xiaochen Bo, Department of Biotechnology, Beijing Institute of Radiation Medicine, Taiping Road 27TH, Haidian District, Beijing 100850, China. Tel.: +86-10-66932251; Fax: +86-10-66931207; E-mail: boxc@bmi.ac.cn; Hui Bai, BioMap (Beijing) Intelligence Technology Limited, N801, North building, Block C, Rongke Information Center, No. 2 Academy of Sciences South Road, Haidian District, Beijing 100005, China. Tel.: +86-10-66930283; E-mail: huibai13@hotmail.com; Xunlong Shi, Department of Biological Medicines, School of Pharmacy, Fudan University, 826 Zhangheng Road, Shanghai 201203, China. Tel.: +86-21-54237431; Fax: +86-21-51980037; E-mail: xunlongshi@fudan.edu.cn
†These authors contributed equally to this work.

Abstract

Inhibition of host protein functions using established drugs produces a promising antiviral effect with excellent safety profiles, decreased incidence of resistant variants and favorable balance of costs and risks. Genomic methods have produced a large number of robust host factors, providing candidates for identification of antiviral drug targets. However, there is a lack of global perspectives and systematic prioritization of known virus-targeted host proteins (VTHPs) and drug targets. There is also a need for host-directed repositioned antivirals. Here, we integrated 6140 VTHPs and grouped viral infection modes from a new perspective of enriched pathways of VTHPs. Clarifying the superiority of nonessential membrane and hub VTHPs as potential ideal targets for repositioned antivirals, we proposed 543 candidate VTHPs. We then presented a large-scale drug–virus network (DVN) based on matching these VTHPs and drug targets. We predicted possible indications for 703 approved drugs against 35 viruses and explored their potential as broad-spectrum antivirals. *In vitro* and *in vivo* tests validated the efficacy of bosutinib, maraviroc and dextromethorphan against human herpesvirus 1 (HHV-1), hepatitis B virus (HBV) and influenza A virus (IAV). Their drug synergy with clinically used antivirals was evaluated and confirmed. The results proved that low-dose dextromethorphan is better than high-dose in both single and combined treatments. This study provides a comprehensive landscape and optimization strategy for druggable VTHPs, constructing an innovative and potent pipeline to discover novel antiviral host proteins and repositioned drugs, which may facilitate their delivery to clinical application in translational medicine to combat fatal and spreading viral infections.

Keywords: virus–host interactome, network analysis, drug target, drug repositioning, antiviral drugs

Introduction

Unexpected regional outbreaks of acute viral infections and the increasing number of chronic viral infections worldwide are still one of the major threats to public health, causing millions of deaths each year [1–4]. The sudden outbreak and global spread of corona virus disease 2019 (COVID-19) is one of the greatest threats worldwide and has caused severe social and economic costs [5]. However, there is no effective treatment or vaccine for many of the highly infectious and pathogenic viruses.

The past 30 years have witnessed extraordinary progress in antiviral drug development. Since 1990, a total of 84 new drugs have been officially approved for clinical antiviral therapies. However, they are only used in the treatment of nine viruses [6] and lack structure diversity, which greatly limits the pipeline of antivirals with new pharmacological mechanisms. Traditional antiviral drug development paradigm focuses on targeting conserved viral genes whose protein products are essential for viral survival or replication. It has major drawbacks including relatively small genomes of viruses providing a limited number of available targets, and constant emergence of drug-resistant variants.

As the importance of host cell functions in viral pathogenicity is increasingly recognized, knowledge of virus–host protein interactions continues to accumulate. These resources may help identify novel molecular targets for antiviral drug discovery and explore mechanisms

Dafei Xie works at Beijing Institute of Radiation Medicine.
Song He works at Beijing Institute of Radiation Medicine.
Lu Han works at Beijing Institute of Pharmacology and Toxicology.
Lianlian Wu is a masters student in Academy of Medical Engineering and Translational Medicine, Tianjin University.
Hai Huang works at the Department of Biological Medicine, School of Pharmacy, Fudan University.
Huan Tao works at Beijing Institute of Radiation Medicine.
Pingkun Zhou works at Beijing Institute of Radiation Medicine.
Xunlong Shi is an associate professor at the Department of Biological Medicine, School of Pharmacy, Fudan University.
Hui Bai is a senior scientist at the Department of Disease Biology in BioMap (Beijing) Intelligence Technology Limited.
Xiaochen Bo is a professor at the Beijing Institute of Radiation Medicine.
Received: November 23, 2021. **Revised:** January 26, 2022. **Accepted:** January 28, 2022

of virus–host interactome [7, 8]. Sufficient evidence shows that drug repositioning, using known small-molecule compounds to target (multi) functional host proteins has excellent safety profiles [9] and promising antiviral effects. It may provide a higher barrier to the development of resistance, as host proteins do not normally mutate in response to therapies [10]. Accordingly, more antiviral drug discovery initiatives are incorporating this attractive approach because it reduces costs and risks of early drug development [11] and expedites the approval of new antiviral indications for old drugs [12]. Current drug repositioning methods include computational approaches, biological experimental approaches and their combination [13]. Computational approaches can be divided into different groups, that is drug-centric, target-based, knowledge-based, signature-based and pathway/network-based methods [14]. Machine learning-based prediction models and frameworks were established in drug discovery using structures and molecular properties of compounds [15–17]. Network analysis-based workflows were also developed to predict potential drug-target interactions, which provided clues for drug repositioning [18–20]. Successful examples include the indications of Gleevec (Abl tyrosine kinase inhibitor) for poxvirus infection [21], U0126 (MEK kinase inhibitor) for influenza virus infection [22], FTI-277 (farnesyltransferase inhibitor) for hepatitis delta virus (HDV) infection [23] and combination of decitabine and gemcitabine (2 antimetabolites) for human immunodeficiency virus (HIV) infection [24]. Recently, computational approaches proposed repositioned drug candidates niacin [25], chloroquine [26, 27], ribavirin and arbidol [28, 29] against COVID-19. Phosphoproteomic analyses also identified 87 Food and Drug Administration (FDA)-approved drugs for the treatment of COVID-19 [30].

On the other hand, many studies focused on a particular viral species or family, and meta-analyses of the host factor sets collected from discrete researches emphasized a low level of congruity. Moreover, in many cases, the identified candidate host targets were not immediately tested by known inhibitors to prove their effectiveness and assess their repositioning potential [4, 31, 32]. This fails to answer a key question, that is, whether the resulting bioinformatic short list of host factors contains suitable candidates for antiviral drug development. Therefore, it is necessary to combine host factor optimization with experimental validation to address the great challenge of moving from systematic evaluation of all host factor data to comprehensive interpretation of their significance and feasibility as antiviral drug targets, to provide promising repositioned drugs for preclinical validation.

In this study, we used this strategy to perform a large-scale landscape investigation. First, we established a systematic overview and statistic of known virus–host protein relationships to provide a global view of human cellular processes that are controlled by viruses, respond to and finally affect viral pathogenicity. Then, we built a network of drug–virus relationships by matching all known specific viruses and approved drugs based on their shared host factors. Instead of examining a single virus or drug, we focused on the overall integration and prediction across all the available drugs and viral pathogens. Immediate cytological and animal tests were conducted for some of the candidates. In summary, we verified that the repositioned drugs bosutinib, maraviroc and dextromethorphan were effective against human herpesvirus 1 (HHV-1), hepatitis B virus (HBV) and influenza A virus (IAV), respectively. We also simulated their effects in combination with antivirals in clinical use today, proving that this strategy can efficiently uncover new host-directed antiviral uses for approved drugs.

Results

Virus-targeted host proteins (VTHPs) can distinguish different viral infections

Virus–host interactome data were collected from VirHostNet and VirusMentha databases, which provided comprehensive and standard data of high quality [7]. A total of 6140 virus-targeted host proteins (VTHPs) have been reported for 151 viruses, including 3 ssDNA viruses, 53 dsDNA viruses, 67 ssRNA viruses, 5 dsRNA viruses and 23 retro-transcribing viruses (Website Table 1; all website tables and datasets are available in http://www.idrug.net.cn/data/Website/index.html). These viruses were named according to the rules of International Committee on Taxonomy of Viruses (ICTV, https://ictv.global/taxonomy/). As shown in Figure 1A, the average number of VTHPs for 151 viruses was 103, and the VTHPs were less than 70 for 116 viruses (76.82%). Notably, the top three ranked viruses with most VTHPs were influenza A virus H1N1 subtype (IAV H1N1, 2271), human immunodeficiency virus 1 (HIV1, 1191) and human herpesvirus 4 (HHV-4, 1108).

In total, these viruses and proteins created 15 583 virus–host protein interactions (Website Table 1). As shown in Figure 1B, the numbers of VTHPs targeted by different numbers of viruses had exponential distribution. There were 3087 (50.28%) VTHPs targeted by single viruses. It should be noted that 15 VTHPs were targeted by >15 viruses, including EEF1A1 (25), HSPA5 (24), TUBA1C (23) *etc*. We found that highly targeted VTHPs were prevailingly cytoskeleton proteins, cell transcription regulation-related proteins, energy metabolism-related proteins and ubiquitin-regulated proteins.

In order to clarify functional relationship between VTHPs in different viral infections, we performed signaling pathway enrichment analyses on 3053 VTHPs targeted by at least two viruses. We found that the most enriched signaling pathways included viral carcinogenesis (127, q-value = $6.46e^{-34}$), Epstein–Barr virus infection (122, q-value = $2.53e^{-30}$), ribosome (93, q-value = $4.44e^{-23}$),

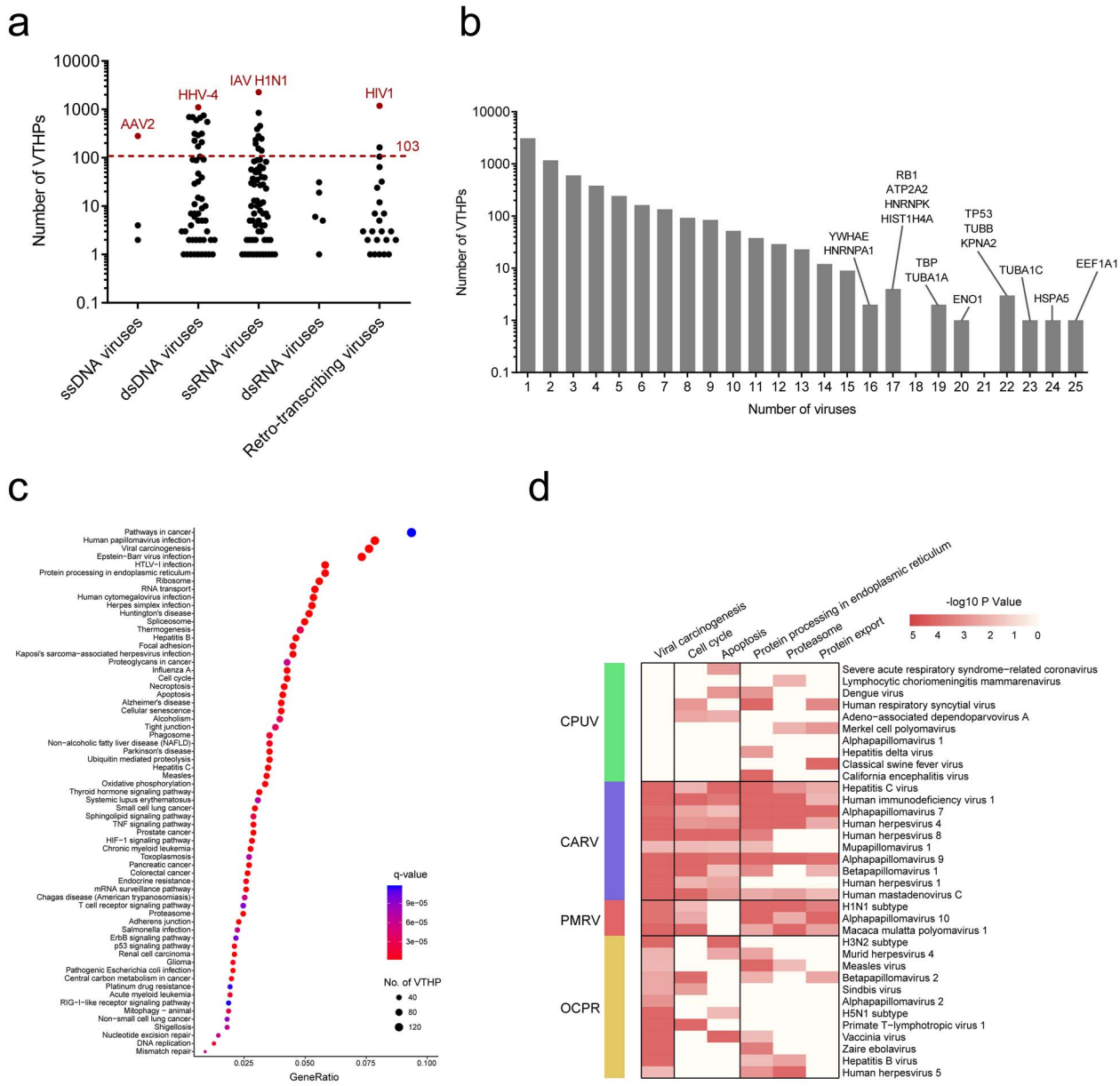

Figure 1. Statistics and enrichment analyses of identified virus-targeted host proteins (VTHPs). (**A**) Distribution of numbers of VTHPs for viruses in Baltimore groups. The red dotted line refers to the average. AAV2, HHV-4, IAV H1N1 and HIV1 refer to adeno-associated dependoparvovirus A, human herpesvirus 4, influenza A virus H1N1 subtype and human immunodeficiency virus 1, respectively. (**B**) Distribution of numbers of VTHPs targeted by different numbers of viruses. (**C**) Enriched signaling pathways of VTHPs targeted by at least two viruses according to Kyoto Encyclopedia of Genes and Genomes (KEGG). (**D**) Clustering of 35 viruses with >70 identified VTHPs according to typical enriched signaling pathways of their VTHPs. The hot map was generated by *R* package pheatmap and colored according to logarithmic *P*-value of enrichment score of each virus.

protein processing in endoplasmic reticulum (97, *q*-value = $1.15e^{-22}$) and spliceosome (83, *q*-value = $1.62e^{-21}$) (Figure 1C, Website Table 2).

Pathway enrichment analyses were further performed using 5956 VTHPs targeted by 35 viruses that had >70 identified VTHPs. Based on typical enrichment of their VTHPs, these viruses can be classified into four groups (Figure 1D, Table S1 available online at http://bib.oxfordjournals.org/). The VTHPs of 10 viruses, including severe acute respiratory syndrome-related coronavirus (SARS-CoV), lymphocytic choriomeningitis mammarenavirus (LCMV) and dengue virus (DENV), are not enriched in any cancer-related pathways. They are defined as cancer pathway unrelated viruses (CPUV). IAV H1N1, alphapapillomavirus 10 and *Macaca mulatta* polyomavirus 1 (SV40) are clustered together as protein metabolism-related viruses (PMRV). As their VTHPs are enriched in pathways of cell cycle and apoptosis, 10 viruses including hepatitis C virus (HCV), HIV1 and alphapapillomavirus 7 are clustered together. They belong to the cell cycle and apoptosis-related viruses (CARV). As other carcinogenic pathway-related viruses (OCPRV), 12 viruses including influenza A virus H3N2 subtype (IAV H3N2), Murid herpesvirus 4 (MuHV-4) and measles virus (MV) are defined. Classification from the perspective of VTHPs is different from traditional

principles. The results highly indicate that VTHP-based antiviral target discovery and drug repositioning require further systematic optimization.

Optimization of druggable VTHPs provides primary candidate targets

In order to evaluate repositioning potential of VTHPs as drug targets, we integrated and investigated the approved/experimental human drug–target relationship in DrugBank database. For the 35 viruses mentioned above, 1149 VTHPs have been proved to be known drug targets (defined as druggable VTHPs), accounting for only 19.29% of their total VTHPs (Website Table 3). The average proportion of druggable VTHPs for the 35 viruses is 25.83% (Figure S1A and sheet of '35 viruses' in Table S2 available online at http://bib.oxfordjournals.org/). The frequencies and average proportions of druggable VTHPs in the 4 groups of viruses are different. The highest proportion was obtained in CPUV (27.33%, sheet of '4 groups' in Table S2 available online at http://bib.oxfordjournals.org/). These limited druggable VTHPs still need to be prioritized. Functionally significant proteins need to be screened out as candidate targets for repositioned antiviral drugs.

Essential gene-encoded proteins (EGEPs) in druggable VTHPs

Wang *et al*. identified 1878 essential genes in more than 20 000 ones in human genome, which have been proved crucial for cell survival and knockout of them can lead to direct cell death [33, 34]. It is noteworthy that viruses may hijack these EGEPs, leading to severe or lethal symptoms. Drugs that directly target them may cause serious side effects or specific toxicity [35]. Therefore, we examined the enrichment of EGEPs in known drug targets and VTHPs of the 35 viruses. We found that 10.35% of the investigated drug targets were EGEPs (P-value = 1.87×10^{-8}) whereas 16.67% of VTHPs were EGEPs (P-value = 8.86×10^{-185}). As shown in Figure S1B, available online at http://bib.oxfordjournals.org/, this ratio is still much lower than that in druggable VTHPs of the 35 viruses (29.30% on average). The top two viruses for most EGEPs are LCMV (54.93%) and Zaire Ebola virus (ZEBOV, 52.94%). Both of them have been proved pernicious and virulent with high fatality rates [36–39]. Meanwhile, vaccinia virus (VacV, 10.53%), MuHV-4 (9.76%) and HDV (0) had the lowest proportions of EGEPs and caused persistent, moderate and mild infections [40–42]. In conclusion, EGEPs are not suitable for drug repositioning.

Membrane proteins in druggable VTHPs

Membrane proteins are important determinants of viral infections and potential appropriate drug targets for effective blocking of viral entry and subsequent signal transduction [43, 44]. Drug–membrane interactions are also significant in medicinal chemistry because compounds enter cells via membrane proteins. Therefore, we examined enrichment of membrane proteins (including plasma membrane, organelle membrane and endoplasmic reticulum membrane proteins) in known drug targets and druggable VTHPs for the 35 viruses.

It is shown that drug targets were significantly enriched in membrane proteins (55.01%, P-value = 2.63×10^{-62}). The proportion of membrane proteins in druggable VTHPs was 52.22% (P-value = 6.69×10^{-17}). The average proportion of membrane proteins in druggable VTHPs of the 35 viruses was 52.94%. Proportions of membrane proteins in five viruses are above 70% (Figure S1C available online at http://bib.oxfordjournals.org/). Therefore, membrane proteins are ideal targets for developing repositioned antiviral therapeutics.

Hub proteins in druggable VTHPs

In human protein–protein interaction (PPI) network, functionally crucial proteins as hubs tend to participate in more regulations by interacting with more proteins and play important roles in maintaining the network structure. Thus, identification of hub proteins may assist in prioritizing druggable VTHPs as more effective targets.

We constructed a PPI network based on BioGrid database and determined regulatory importance of functional proteins according to their degrees. Using 329 (upper 1% quantile) as threshold, we obtained hub proteins. We found that 2.77% of known drug targets were hubs (P-value = 5.05×10^{-24}) and it was comparable to that in VTHPs (2.50%, P-value = 1.18×10^{-56}). We then investigated druggable VTHPs and found that the proportion of hub proteins was 6.09% (P-value = 3.28×10^{-43}). As shown in Figure S1D, available online at http://bib.oxfordjournals.org/, an average of 15.44% of the druggable VTHPs of the 35 viruses were hub proteins. Human herpesvirus 5 (HHV-5, 32.26%) and sindbis virus (SINV, 30.56%) had proportions of hub proteins above 30%. Hub proteins in druggable VTHPs are potential targets for developing antiviral therapeutics in drug repositioning.

Therefore, we proposed three selection principles for screening suitable VTHPs in antiviral drug repositioning as follows: (1) they should have been proved to be druggable, and (2) they should not be EGEPs, but (3) they should be membrane or/and hub proteins. In total, we obtained 209 EGEPs and 940 nonessential druggable VTHPs for the 35 viruses (Figure 2). Among the latter, 520 (55.32%) were membrane proteins and 48 (5.11%) were hub proteins. There are 25 VTHPs being both membrane and hub proteins. These 543 nonessential druggable membrane or hub proteins are most promising for predicting host-directed repositioned antivirals, which are defined as candidate VTHPs.

Predicting repositioned host-directed antiviral drugs based on optimized VTHPs

We determined the selection criteria for candidate repositioned drugs according to those of VTHPs. Their targets should contain one or more membrane or/and hub protein(s), which are druggable but not EGEPs.

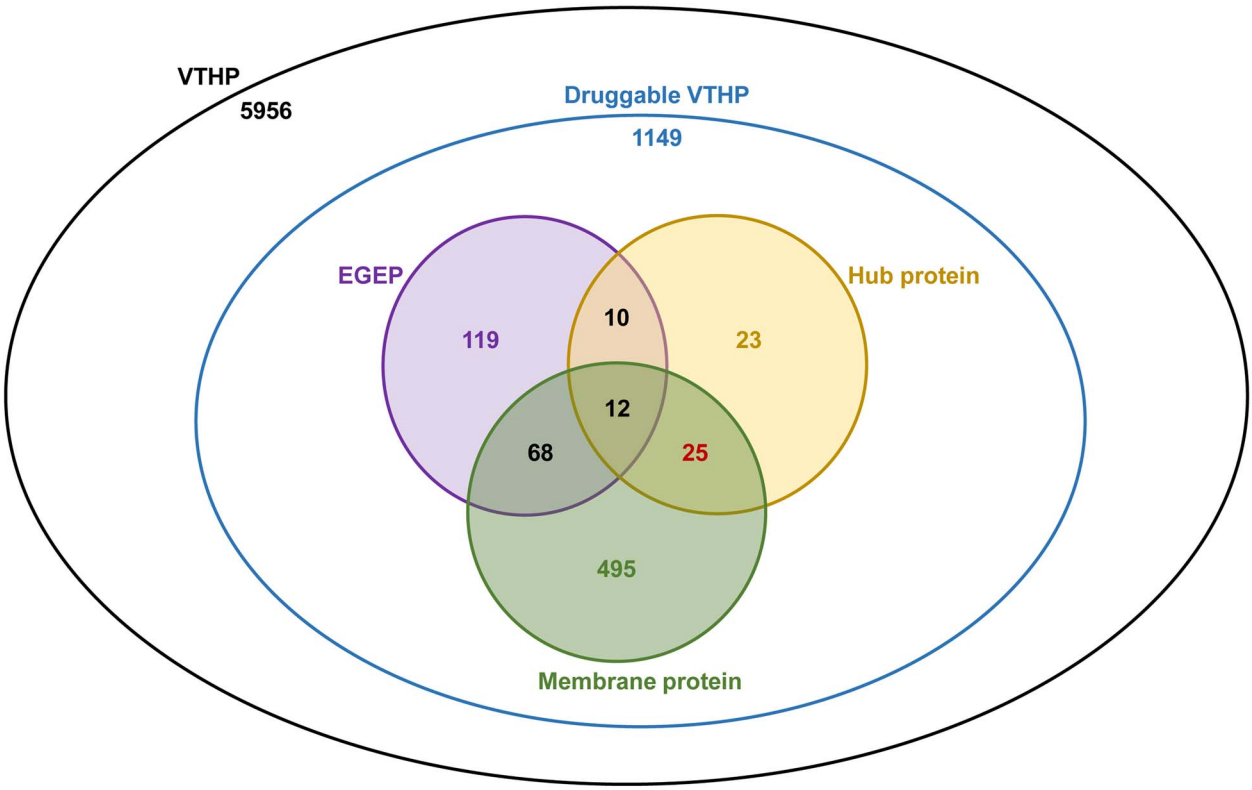

Figure 2. Venn diagram showing distinction and overlap of essential gene-encoded proteins (EGEPs, purple area), membrane proteins (green area) and hub proteins (yellow area) in druggable virus-targeted host proteins (VTHPs). The red number refers to nonessential druggable VTHPs being both membrane and hub proteins.

Through statistics, we found that optimized druggable VTHPs of the 35 viruses could be targeted by 2786 small-molecule compounds. Specifically, approved drugs with more favorable toxicity profiles and recognized effectiveness can greatly reduce preclinical evaluations, representing a preponderant class of drugs for repositioning. Thus, we selected 703 approved drugs targeting 428 candidate VTHPs of the 35 viruses to construct a drug–virus network (DVN) (Figure 3A, Website Table 4). It indicated relationship and attributes of these viruses and the possible drugs which were established through the repositioning strategy that VTHPs of some viruses were also targets of specific drugs. In DVN, there are a total of 3003 drug-virus connections. As shown in Figure 3B, each virus is connected to 87 drugs on average. Alphapapillomavirus 7, 9 and 10 are connected to 300, 264 and 250 drugs, respectively, showing the highest repositioning potential.

Moreover, we tried to determine types of repositioned drugs according to Anatomical Therapeutic Chemical (ATC) classification codes (Figure 3C, sheet of 'ATC codes' in Table S3 available online at http://bib.oxfordjournals.org/). Codes are available for 588 drugs. Among them 178 are used in the nervous system showing 906 connections with 29 viruses. We also found 60 for the alimentary tract and metabolism showing 279 connections with 31 viruses. It suggests that drugs originally developed for the nervous system have the highest antiviral repositioning potential. Types of repositioned drugs for these viruses vary greatly (Table S3 available online at http://bib.oxfordjournals.org/).

We further evaluated possible antiviral spectrums of repositioned drugs by counting numbers of their connected viruses. As shown in Figure 3D, 239 (34.00%) drugs show a single connection with a single virus, presenting specific repositioning relationships. For example, the antiinflammatory agent fluticasone propionate is repositioned for anti-IAV H3N2 for sharing the host target PLA2G4A. In addition, 112 (15.93%) drugs were connected with 2 viruses whereas 10 to 100 drugs were connected with 3 to 11 viruses, accounting for 47.08% of all predicted drugs. Eighteen drugs were connected with more than 14 viruses. Highly connected drugs included copper (31), fostamatinib disodium (29), artenimol (28), zinc acetate (28) and acetylsalicylic acid (28). They hold greater potential to be developed as broad-spectrum antivirals. They are all multitarget drugs repositioned for different viruses through targeting different VTHPs.

Repositioning relationship between a drug and a virus was established by sharing one or more candidate VTHP(s). Therefore, the 3003 drug–virus connections increase to 4138 drug–VTHP–virus connections if we calculate multitarget drugs repositioned for specific viruses by targeting more than 1 VTHPs. As a result, all viruses except classical swine fever virus (CSFV) and

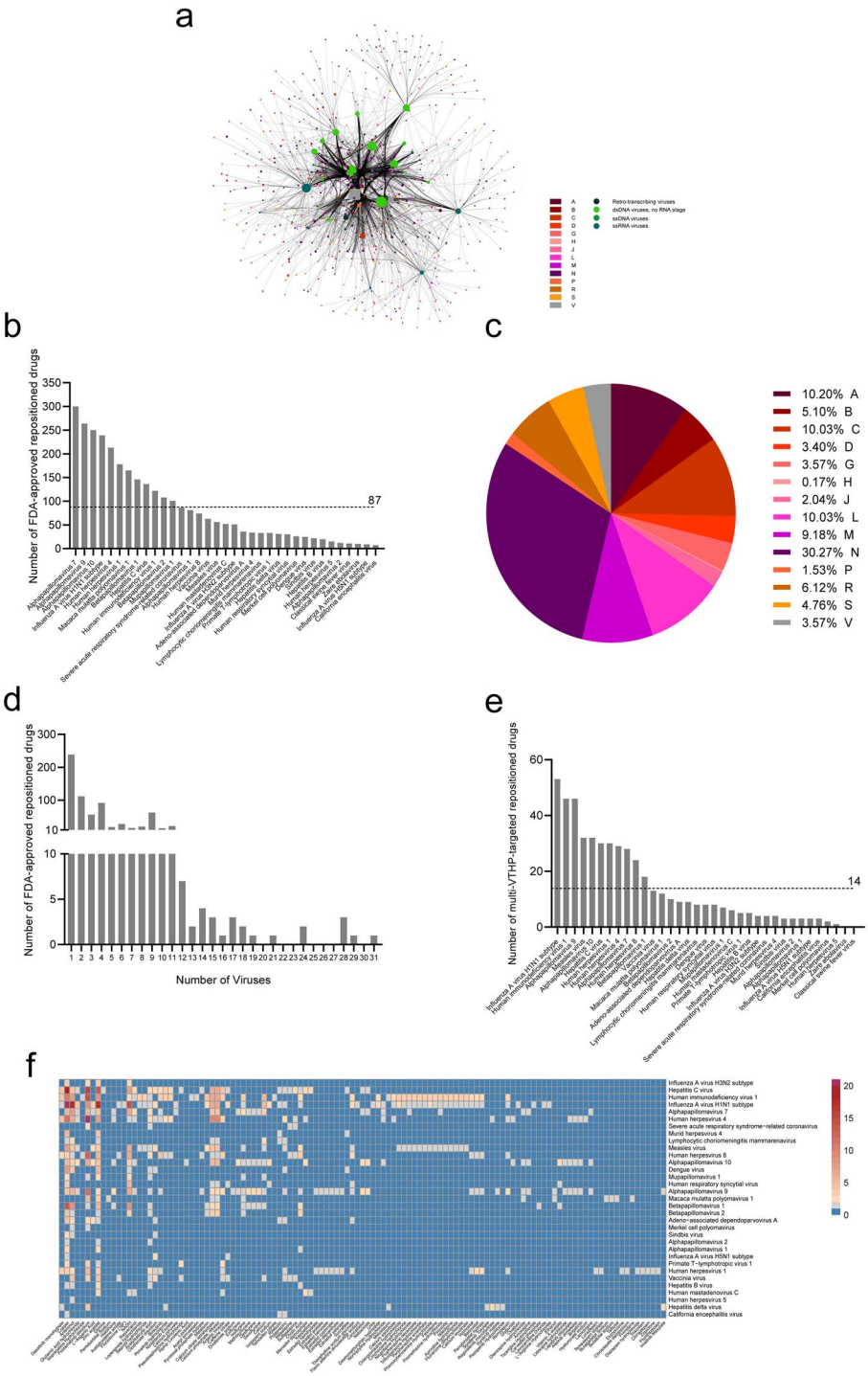

Figure 3. Drug-virus network (DVN) and statistics on 35 viruses with >70 identified virus-targeted host proteins (VTHPs) and their predicted potential repositioned drugs. (**A**) DVN showing possible therapeutic relations among the 35 viruses and 703 approved drugs. A link was placed between a drug and a virus if they shared at least 1 of the 543 candidate VTHPs. Circles represent viruses which are differentially colored according to their Baltimore groups. Squares represent drugs which are differentially colored according to their ATC classification codes. Sizes of circles (viruses) are proportional to numbers of their related drugs whereas sizes of squares (drugs) are proportional to numbers of their identified protein targets according to DrugBank database. (**B**) Statistics on numbers of predicted repositioned approved drugs for the 35 viruses. (**C**) Proportional distribution of different types of predicted repositioned drugs according to ATC classification codes. (**D**) Statistics on numbers of predicted repositioned approved drugs with respect to numbers of viruses. (**E**) Statistics on numbers of multi-VTHP-targeted repositioned drugs for the 35 viruses. (**F**) Heatmap presenting numbers of candidate VTHPs shared by drug–virus pairs. Viruses are listed in rows and drugs are listed in columns. Color blocks indicate numbers of shared candidate VTHPs. Details of ATC codes in **A** and **C** are shown under ATC codes in Table S3 available online at http://bib.oxfordjournals.org/.

ZEBOV were connected to at least 1 repositioned drug by sharing two or more VTHPs. As shown in Figure 3E, average number of multi-VTHP-targeted repositioned drugs for the 35 viruses was 14. IAV H1N1 (53), HIV1 (46) and alphapapillomavirus 9 (46) were the top three viruses with most multi-VTHP-targeted repositioned drugs. Statistically, there were 117 drugs repositioned for 33 viruses by sharing more than 1 VTHPs, which are displayed in a heatmap (Figure 3F). It indicated that the predicted potential broad-spectrum antivirals copper and fostamatinib disodium shared most candidate VTHPs (21) with IAV H1N1 and HHV-4, respectively.

Preclinical validation of host-directed repositioned drugs for antiviral treatments

To further evaluate our optimization strategy and feasibility of DVN for antiviral repositioning, we selected HHV-1, HBV and IAV to validate potential of candidate VTHPs and predicted drugs. HHV-1, HBV and IAV are representative viruses from different Baltimore groups and clusters of enriched VTHPs. Approved host-directed agents against them are currently rare [45, 46]. We extracted a subnetwork for each virus and chose commercially available drugs. Candidates targeted at least 1 nonessential druggable membrane or/and hub protein while controls targeted EGEPs or nonessential, nonmembrane, nonhub VTHPs. We first tested their cytotoxicity and then efficacy at noncytotoxic concentrations. The most potent drugs were further evaluated in combination therapy with commercially available antivirals.

HHV-1 and bosutinib

We identified 227 drugs for anti-HHV-1 repositioning based on 38 candidate VTHPs (Figure 4A), of which 7 were selected for test. In addition, eight drugs targeting EGEPs and nonessential noncandidate VTHPs were used as controls. As shown in Figure 4B, these drugs showed varied toxicities on African green monkey kidney cells (Vero) and the half-toxic concentrations (TC_{50}) ranged from 11.9 to 362.4 μg/ml. Under nontoxic concentrations, their anti-HHV-1 efficacy was evaluated by the cytopathic effect (CPE). Isoprenaline (half-inhibitory concentrations, IC_{50} = 88.8 μg/ml) and bosutinib (IC_{50} = 7.0 μg/ml) showed significant inhibitory effect on CPE. Notably, the Bcr-Abl kinase inhibitor bosutinib showed the strongest inhibitory effect. Its treatment index (TI, 3.61) was higher than that of isoprenaline (2.69).

Using the Loewe additivity model, we assessed the efficacy of combination therapy of bosutinib with acyclovir (ACV), a clinically effective anti-HHV-1 drug. Synergy scores were calculated to accurately indicate synergism (>0) and antagonism (<0). As shown in Figure 4C, drug antagonism was observed over a wide concentration range of the two drugs, resulting in a negative average synergy score of −18.59.

HBV and maraviroc

We predicted 54 drugs for anti-HBV repositioning based on 16 candidate VTHPs (Figure 5A). We selected four drugs targeting candidate VTHPs and five drugs targeting nonessential noncandidate VTHPs for further investigation. As shown in Figure 5B, these drugs showed varied toxicities on hepatoma cell line HepG2.2.15 transfected with HBV genome, and the TC_{50} ranged from 14.0 to 928.4 μg/ml. Under nontoxic concentrations, their anti-HBV efficacy was evaluated by determining surface antigen of HBV (HBsAg) and hepatitis B e-antigen (HBeAg) in culture medium. There were four drugs showing significant inhibitory effect on secretion of HBsAg. IC_{50} was calculated for maraviroc (80.2 μg/ml), melatonin (151.9 μg/ml), etodolac (18.9 μg/ml) and resveratrol (20.4 μg/ml). Notably, maraviroc showed a strong inhibitory effect on HBsAg at various concentrations (Figure 5C) and a TI of 11.10, which was much higher than those of the other three. Meanwhile, four drugs showed weak inhibitory effect on HBeAg, namely acitretin, alitretinoin, etodolac and resveratrol (data not shown). However, their effect was limited at nontoxic concentrations.

We then assessed inhibitory effect of maraviroc on HBsAg, HBeAg and HBV replication in a time-course manner to determine its anti-HBV activity with limited toxicity (Figure 5D). At all 4 concentrations, maraviroc increased HBsAg inhibition in a time-dependent manner. However, the most significant inhibitory effect on HBeAg and HBV-DNA appeared on D3 of treatment regardless of concentrations. These results indicated that maraviroc at single doses could elicit consistent inhibitory effect on HBsAg.

We further explored the efficacy of combined treatment of maraviroc and lamivudine, a clinically effective nonnucleoside reverse transcriptase inhibitor of HBV in a nine-day treatment and evaluated drug synergy using the Loewe additivity model. As shown in Figure 5E (left lane), drug synergy on HBsAg inhibition was demonstrated over a specific concentration range only on D3. Antagonism was observed over a robust concentration range, resulting in negative average synergy scores at all three time points. Similarly, in the middle lane, drug synergy on HBeAg inhibition was observed over a specific concentration range on D3 and D6. Regarding HBV-DNA inhibition in the right lane, drug synergy could only be observed in a limited range. Strong antagonism was demonstrated on D3 and D9, and the average synergy score dropped to −44.405 on D9.

IAV and dextromethorphan

We noticed that 393 drugs were predicted for anti-IAV H1N1 repositioning based on 138 candidate VTHPs, and 80 for anti-IAV H3N2 repositioning based on 19 candidate VTHPs (Figure 6A). There were 61 potential candidates to treat both subtypes. In total, we selected 19 drugs for test against IAV H1N1 (Figure 6B). Dexamethasone, resveratrol, bosutinib, cyclosporine and probucol were also tested against IAV H3N2. They showed various toxicities on the Madin–Darby canine kidney (MDCK) cells and the TC_{50} ranged from 0.305 to 1029.3 μg/ml. At nontoxic concentrations, the anti-IAV H1N1 and H3N2

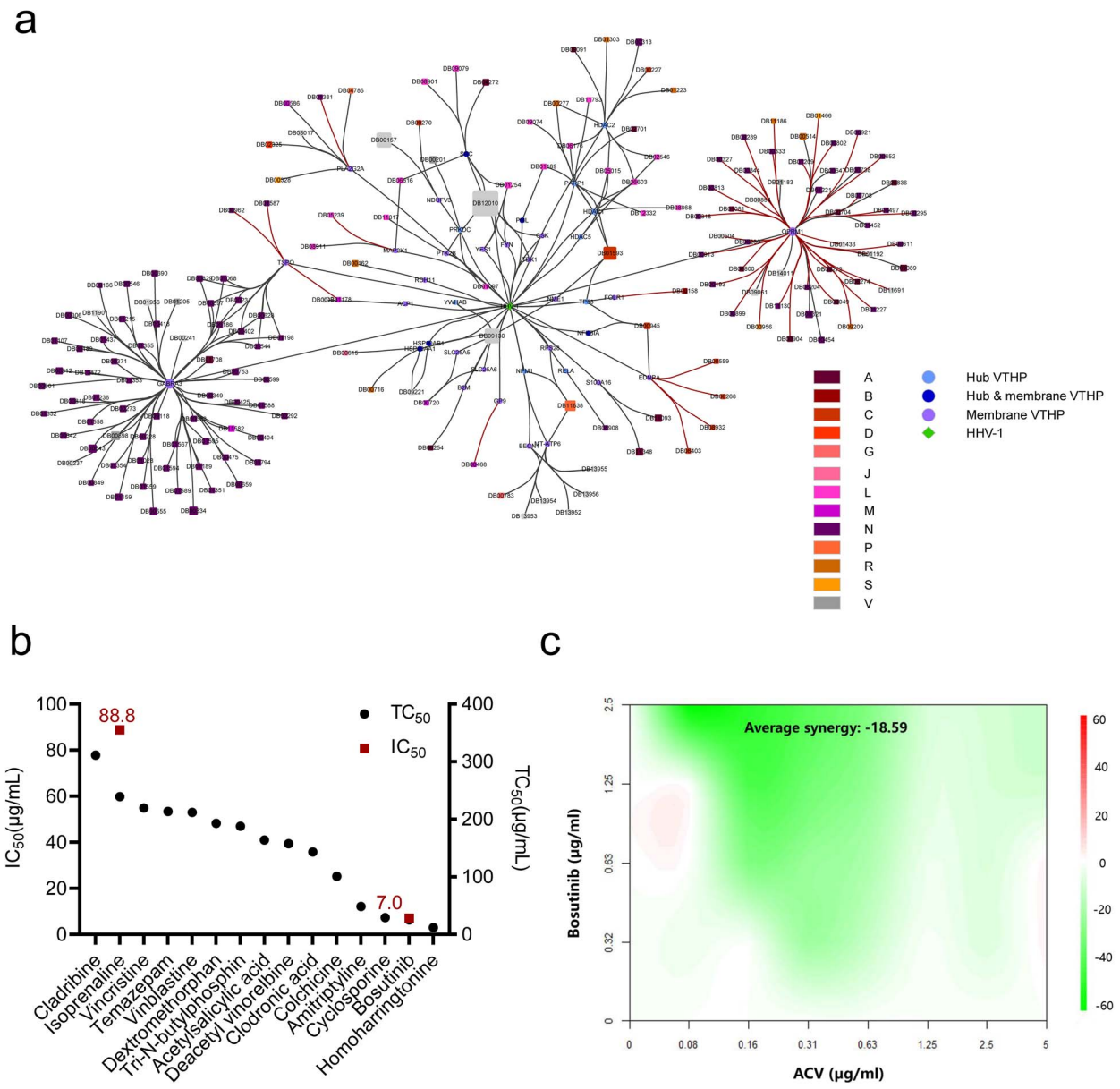

Figure 4. Prediction and verification of potential repositioned antihuman herpesvirus 1 (HHV-1) drugs, of which bosutinib turned to be the most promising one. (**A**) Drug–target–virus network of HHV-1. HHV-1 was connected to all candidate virus-targeted host proteins (VTHPs). A link was placed between a drug and a VTHP if the VTHP has been reported to be 1 of the known targets of the drug according to DrugBank database. Squares represent drugs which are differentially colored according to their ATC classification codes (ATC codes in Table S3 available online at http://bib.oxfordjournals.org/). Sizes of circles (VTHPs) are proportional to numbers of their connected drugs and those of squares (drugs) are proportional to numbers of their identified protein targets according to DrugBank database. (**B**) Half-toxic concentrations (TC_{50}) of 15 tested drugs and half inhibitory concentrations (IC_{50}) of 2 of them showing significant inhibitory effect on cytopathic effect (CPE) under nontoxic concentrations. We found four drugs targeting candidate membrane VTHPs including amitriptyline hydrochloride, clodronate disodium, dextromethorphan hydriodide and temazepam acetate. We also selected valproic acid targeting candidate hub VTHPs. Acetylsalicylic acid and bosutinib target both membrane and hub VTHPs. Meanwhile, we used cladribine, colchicine, vinblastine sulfate, vincristine sulfate, vinorelbin, homoharringtonine, cyclosporine and isoprenaline that target essential gene-encoded proteins (EGEPs) or/and nonessential noncandidate VTHPs as controls. TC_{50} and IC_{50} were obtained from triplicates and representative of two independent experiments. (**C**) Synergy effect of bosutinib and acyclovir (ACV) determined using Loewe additivity model with *R* package SynergyFinder. Synergy scores were evaluated according to dose–response relationships of the two drugs applied respectively or simultaneously. Colors in the landscape indicate synergy scores of the combinations with different concentrations of the two drugs. Red areas (synergy score > 0) represent drug synergy while green ones (synergy score < 0) represent drug antagonism. Absolute values indicate intensity of drug synergy or antagonism. Average synergy score was calculated with the dose matrixes.

efficacy of the drugs were evaluated by determining CPE upon 10 tissue culture infectious dose 50 ($TCID_{50}$) of viral infection. As a result, six and three tested drugs exhibited CPE inhibitory effect in IAV H1N1 and H3N2 infection, respectively, and their CPE inhibition (CPEI) was obtained. Notably, dextromethorphan (25 μg/ml, $CPEI_{H1N1}\% = 37.5\%$, $CPEI_{H3N2}\% = 25\%$), dexamethasone (100 μg/ml, $CPEI_{H1N1}\% = 25\%$, $CPEI_{H3N2}\% = 12.5\%$) and

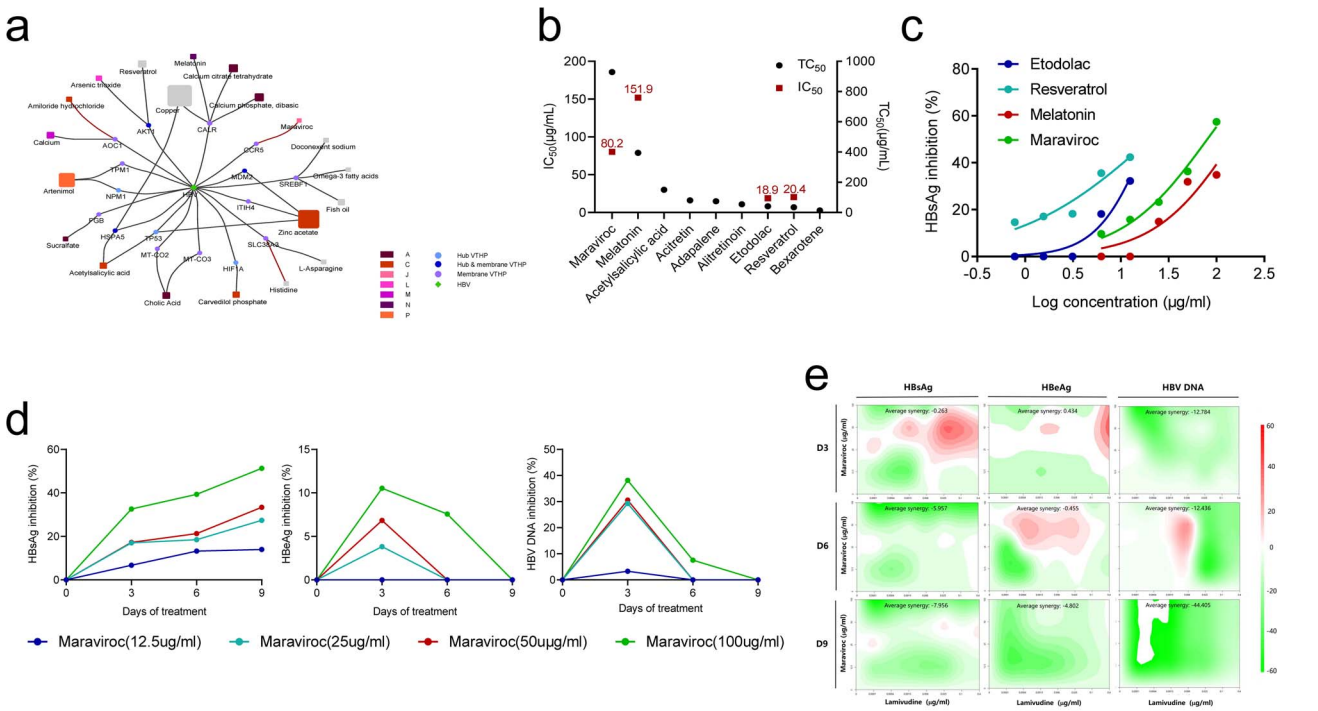

Figure 5. Prediction and verification of potential repositioned antihepatitis B virus (HBV) drugs, of which maraviroc turned to be the most promising one. (**A**) Drug–target–virus network of HBV. HBV was connected to all candidate virus-targeted host proteins (VTHPs). A link was placed between a drug and a VTHP if the VTHP has been reported to be 1 of the known targets of the drug according to DrugBank database. Squares represent drugs which are differentially colored according to their Anatomical Therapeutic Chemical (ATC) classification codes (ATC codes in Table S3 available online at http://bib.oxfordjournals.org/). Sizes of circles (VTHPs) are proportional to numbers of connected drugs and those of squares (drugs) are proportional to numbers of their identified protein targets according to DrugBank database. (**B**) Half-toxic concentrations (TC_{50}) of nine tested drugs and half inhibitory concentrations (IC_{50}) of four of them showing significant inhibitory effect under nontoxic concentrations. We selected maraviroc and melatonin targeting candidate membrane VTHPs. Acetylsalicylic acid and resveratrol targeted both membrane and hub VTHPs. Adapalene, bexarotene, acitretin, alitretinoin and etodolac targeting nonessential noncandidate VTHPs were used as controls. (**C**) Inhibitory effect on secretion of HBsAg of the four drugs with respect to their logarithmic concentrations. (**D**) Inhibitory effect on secretion of HBsAg, HbeAg and HBV replication of maraviroc in different concentrations with respect to days of treatment. HBsAg inhibition increases to 13.99%, 27.38%, 33.39% and 51.27% for the four concentrations of maraviroc on D9, respectively. HBeAg inhibitions at concentrations of 25–100 μg/ml grow in the first 3 days of treatment, followed by a decline. HbeAg inhibition decreases to 0 on D9 at 100 μg/ml and on D6 at lower concentrations. Note that on D3 maraviroc at the highest concentration (100 μg/ml) shows 10.53% and 38.13% inhibitions on HBeAg and HBV replication, respectively. (**E**) Synergy effect of maraviroc and lamivudine analyzed using Loewe additivity model with *R* package SynergyFinder. Synergy scores were evaluated according to dose–response relationships of the two drugs applied respectively or simultaneously. Colors in the landscapes indicate synergy scores of the combinations with different concentrations of the two drugs. Red areas (synergy score > 0) represent drug synergy while green ones (synergy score < 0) represent drug antagonism. Absolute values indicate intensity of drug synergy or antagonism. Average synergy scores were calculated with the dose matrixes. Data of *in vitro* tests were obtained from triplicates and representative of two independent experiments.

resveratrol (12.5 μg/ml, $CPEI_{H1N1}\% = 25\%$, $CPEI_{H3N2}\% = 12.5\%$) showed CPEI upon both subtypes. However, IC_{50} was only calculated for dextromethorphan (22.2 μg/ml) and atomoxetine (44.4 μg/ml) after IAV H1N1 infection. Other drugs could not be evaluated due to their low efficacy.

We compared the inhibitory effect of dextromethorphan and atomoxetine combined with oseltamivir in both short-term high-dose (48 h, 100 $TCID_{50}$) and long-term low-dose (72 h, 10 $TCID_{50}$) infection modes *in silico* on CPEI (Figure 6C). Robust drug synergy for dextromethorphan + oseltamivir in short-term high-dose mode was observed over a wide concentration range, with an average synergy score of 0.814. An even higher average synergy score was obtained in long-term low-dose mode. However, antagonism was observed for atomoxetine + oseltamivir over a full tested concentration range in both modes, and their average synergy scores were negative.

Dose–response experiments were performed to investigate protection of dextromethorphan + oseltamivir against IAV H1N1 in a murine model. Mice infected with a lethal dose of virus showed severe clinical manifestations on D3 after infection. We found that 62.5% of the infected mice that received the placebo died on D6, and mice in most of treatment groups had higher survival rates. Notably, 12.5% of the mice in dextromethorphan + oseltamivir (15 mg/kg/d + 15 mg/kg/d) group survived to D11 after infection. It was also noteworthy that no matter in single or combined treatments higher doses (30 and 60 mg/kg/d) of dextromethorphan were less effective than a lower dose (15 mg/kg/d). By D9 all mice taking placebo died whereas mice taking oseltamivir (15 mg/kg/d) and dextromethorphan + oseltamivir (15 mg/kg/d + 15 mg/kg/d) had the survival rates of 37.5% and 50.0%, respectively (Figure 6D). Body weights of infected mice in both control and treatment groups kept decreasing from D3 and

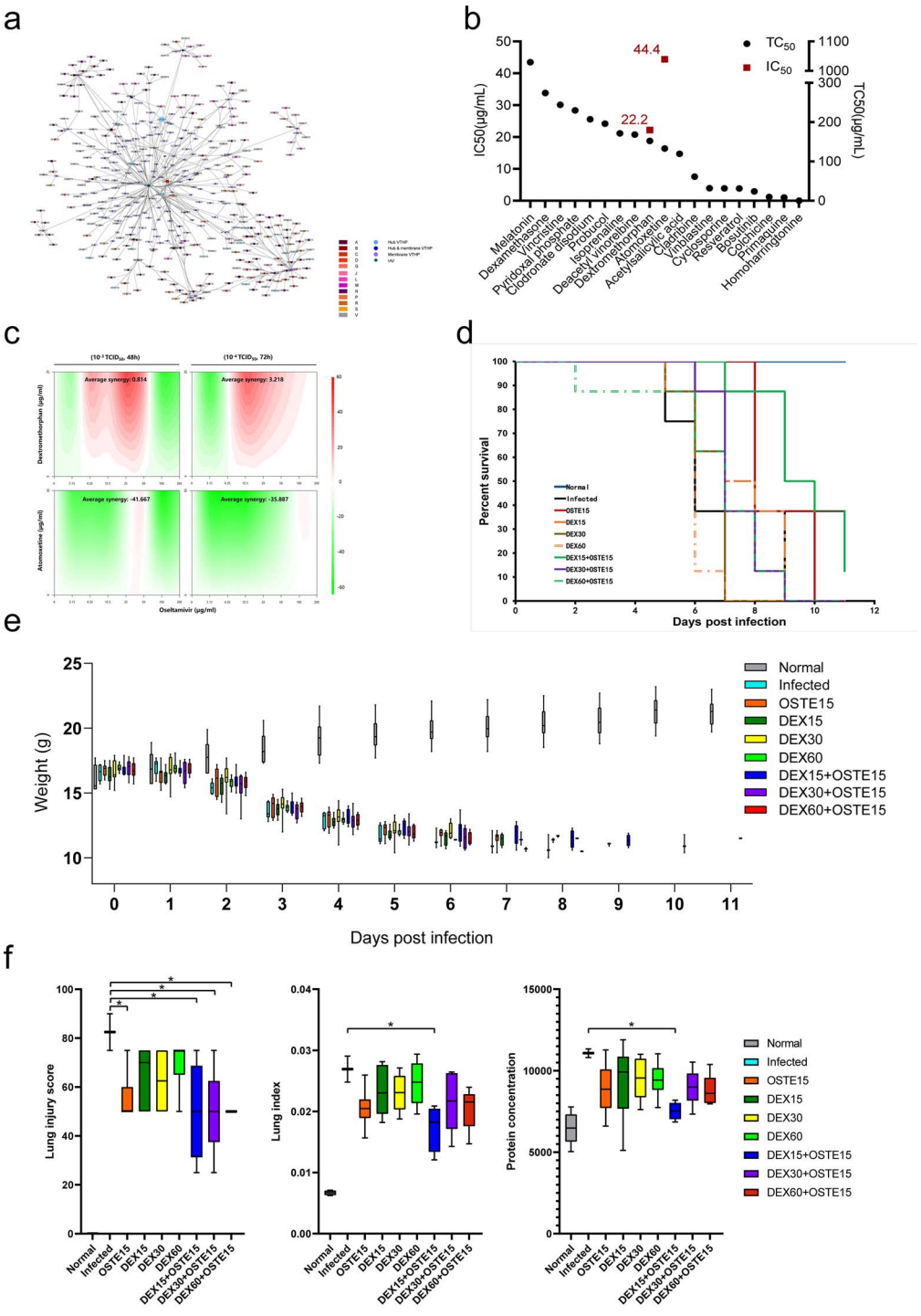

Figure 6. Prediction and verification of potential repositioned anti-influenza A virus (IAV) drugs, of which dextromethorphan turned to be the most promising one. (**A**) Drug–target–virus network of IAV H1N1 and H3N2. The two subtypes of IAV were connected to their candidate virus-targeted host proteins (VTHPs). A link was placed between a drug and a VTHP if the VTHP has been reported to be one of the known targets of the drug according to DrugBank database. Squares represent drugs which are differentially colored according to their ATC classification codes (ATC codes in Table S3 available online at http://bib.oxfordjournals.org/). Sizes of circles (VTHPs) are proportional to numbers of connected drugs and those of squares (drugs) are proportional to numbers of their identified protein targets according to DrugBank database. (**B**) Half-toxic concentrations (TC_{50}) of 19 tested drugs and half inhibitory concentrations (IC_{50}) of dextromethorphan and atomoxetine showing significant cytopathic effect (CPE) inhibitory effect under nontoxic concentrations. Among them dextromethorphan targets candidate membrane VTHPs PGRMC1, RAC1 and CYBA against IAV H1N1. Dexamethasone targets membrane VTHP ANXA1 against both subtypes. Bosutinib targets both membrane and hub VTHP SRC against IAV H1N1 and essential gene-encoded protein (EGEP) BCR against IAV H3N2. Cyclosporine and probucol are controls targeting nonessential noncandidate VTHPs PPIA and CES1, respectively, against both subtypes. (**C**) Landscapes representing predicted synergy effect of atomoxetine and dextromethorphan combined with oseltamivir analyzed by R package SynergyFinder based on the Loewe additivity model. Synergy scores were evaluated according to dose–response relationships of the two drugs applied respectively or simultaneously. Colors in the landscapes indicate synergy scores of the combinations with different concentrations of the two drugs. Red areas (synergy score > 0) represent drug synergy while green ones (synergy score < 0) represent drug antagonism. Absolute values indicate intensity of drug synergy or antagonism. Average synergy scores were calculated with the dose matrixes. (**D**) Survival of IAV H1N1-infected mice with respect to time post infection. (**E**) Body weights of IAV H1N1-infected mice with respect to time post infection. (**F**) Lung injury scores (left), lung indexes (middle) and protein concentrations (right) of IAV H1N1-infected mice treated with different doses of dextromethorphan, oseltamivir and their combinations. Data were obtained from triplicates and representative of two independent experiments.

sustained at low levels until the end of the experiment (Figure 6E). The treatments failed to restore the weights to the normal level. In addition, oseltamivir (15 mg/kg/d) alone or in combination with dextromethorphan could relieve lung injury induced by viruses. Pathology examinations showed that dextromethorphan + oseltamivir at all three doses significantly decreased lung injury scores (Figure 6F, left). Only dextromethorphan + oseltamivir (15 mg/kg/d + 15 mg/kg/d) significantly decreased lung index (0.017, Figure 6F, middle) and protein concentration in lungs (7522.13, Figure 6F, right), which were 0.007 and 6484.80 in model group, respectively. These results indicated that dextromethorphan + oseltamivir (15 mg/kg/d + 15 mg/kg/d) prolonged survival time of mice and ameliorated pathological changes in lungs caused by viral infection. This combination demonstrated potent therapeutic effect against IAV H1N1 *in vivo*, and it is superior to single or combined treatments of dextromethorphan at higher doses.

Discussion

The prevailing paradigm for drug discovery, including antivirals, is extremely time-consuming, expensive and risky [47]. Drug repositioning reduces the time and cost and advances delivery of new drugs to patients in urgent need [48]. In addition to economic considerations, host-directed antiviral strategy aims to enhance protective responses of hosts, reduce severe inflammation and balance immune reactions [49]. It has been proved to be especially attractive for the fast development of antiviral therapeutics in control of severe or acute infectious disease outbreaks such as COVID-19.

In general, candidate VTHPs and therefrom repositioned drugs in this study were screened out through four steps. First, druggable VTHPs had a priority and leading role for their larger probabilities of being potential repositioned drug targets, providing a broad space for host-directed drug development. Next, we ruled out EGEPs from druggable VTHPs so that repositioned drugs would not cause critical adverse drug reactions. Then, we indicated that membrane and hub proteins tended to be ideal targets for antiviral repositioning. It is possible that membrane proteins are more potential candidates for they outnumber hub proteins by more than 10 times (520/48). Finally, DVN was constructed based on a comprehensive investigation of drug–virus interactions. We emphasized potency of optimized targets and their corresponding repositioned drugs by comparing them with drugs targeting essential or nonessential noncandidate VTHPs. We found that drugs for the nervous system had the greatest promise in antiviral repositioning strategy. Copper and fostamatinib disodium were likely to be potential broad-spectrum antivirals. However, their interactions with different viruses were complicated and inconsistent, implying further exploration and deeper insights into broad-spectrum antivirals discovery. We extracted subnetworks from DVN and selected potential repositioned drugs bosutinib against HHV-1, maraviroc against HBV and dextromethorphan against IAV for tests. The following results were obtained from the *in vitro* tests: (1) The representative optimized repositioned drugs including bosutinib, maraviroc and dextromethorphan showed evident antiviral effect. Membrane VTHPs were found in all the three viruses. (2) Targeting hub VTHPs also inhibited proliferation of viruses in many cases. (3) Repositioned drugs related to viruses via nonessential noncandidate VTHPs tended to show weak inhibitory effect on the pathogens. (4) Compounds targeting EGEPs showed stronger cell toxicity, implying more serious adverse drug reactions. In addition, we found that lower doses of dextromethorphan were more efficient in inhibiting IAV replication than higher doses. Notably, most drug–virus connections shared multitargets and these multi-VTHP-targeted repositioned drugs may be considered to have greater chances as antivirals.

Our results demonstrated that this comprehensive computational pipeline significantly expanded drug candidate repertoires beyond virus-directed strategy. The set of membrane and hub VTHPs offers crucial clues for drug candidate prioritization. Excluding EGEPs and prioritizing membrane and hub VTHPs will increase success rates in drug target identification and antiviral development, which highlights the superiority and significance of our strategy. Besides, the network analyses in this study further supported use of PPI during candidate prioritization in identifying important host factors as potential therapeutic targets.

It is well recognized that host-directed therapy should be a synergistic complement to canonical antivirals and become indispensable [50]. Combined strategies of host-directed drugs and existing ones, or drugs with various targets provide greater prospects and will play more important roles in infectious disease treatment as they could improve the efficacy at lower doses. It is worth noting that drug combination is one of the hot topics and has been extensively studied for their potential efficiency in treatment of COVID-19 [51–53]. We therefore evaluated combined therapies and observed synergistic effect of drug combinations tested on three different viruses. For dextromethorphan against IAV *in vivo*, the combination with oseltamivir showed apparent antiviral effect at lower dosages of dextromethorphan with fewer side effects. Robust drug synergy was found in both short-term high-dose and long-term low-dose modes in wider concentration ranges. However, the combination of bosutinib with ACV against HHV-1 exhibited drug synergy only in a limited concentration range whereas drug antagonism was observed widely. Similarly, anti-HBV combination of maraviroc and lamivudine also showed synergistic effect in specific and limited concentration ranges. Results of combined therapies of predicted host-directed antivirals and existed ones were inferred to be complicated and unpredictable, which suggested careful consideration and balancing. Moreover, possible drug–drug interactions and the resulting adverse effects [54]

should also be considered. Future treatment regimens with appropriate collocation of virus-directed and host-directed multitarget drugs would provide the best possible combinations.

More work is still needed in the identification and verification of potential host-directed antiviral targets and repositioned drugs. In future work, network construction will evolve with rapid accumulation of data on host factors and drug targets. Information from a large number of reports and databases extracted by text mining using intelligent computational methods should also be integrated for heterogenous consideration [55–58]. Additional network analyses would be performed in DVN. Another significant topic is development of broad-spectrum antivirals. Identification of host cell factors and pathways that are commonly used by different viruses may lead to the discovery of new broad-spectrum antivirals. Overall, although the efficacy of candidate drugs still needs further validation, the systematic analyses and prioritization of host-directed targets and the repositioning strategy in this study have shown potent predictive power for target and drug discovery as an integral component in small-molecule antiviral drug research and development.

Methods and materials

Data source and data preprocessing

We collected 22 278 and 10 692 Virus-host PPIs (VH-PPIs) from VirHostNet and VirusMentha databases, respectively (Website Dataset 1). The data of VH-PPIs were preprocessed in three steps. First, redundant PPIs reported by the same literature were integrated. Second, items of viruses without definitions in taxonomy were removed. Third, two bacteriophages were removed. The final VH-PPI data contained a total of 28 849 nonredundant PPIs (Website Table 1). We also obtained 13 441 drug–target relations among 4773 approved/experimental drugs and 2672 target proteins in human from DrugBank database (Website Dataset 2).

EGEPs were collected from the research of Wang *et al*. [33] according to the recommended threshold. We scanned and screened Gene Ontology (GO) database and proteins encoded by genes in the cellular component terms 'membrane', 'plasma membrane', 'endoplasmic reticulum membrane' and 'organelle membrane' were defined as membrane proteins in this study. Human PPI network was constructed according to data from BioGrid database. We considered proteins whose degrees ranked the upper 1% quantile in the network as hub proteins.

In this study, we used Target Uniprot ID as the identifier for host factors and drug targets.

Clustering of virus-targeted host proteins (VTHPs) based on pathway enrichment analyses

Pathway enrichment analyses of VTHPs were performed based on Kyoto Encyclopedia of Genes and Genomes (KEGG), which provides tools for understanding and representation of biological systems and processes. We established four clusters including CPUV, CARV, PMRV and OCPRV according to three criteria: (1) whether a virus could be enriched in cancer-related pathways, (2) whether a virus could be enriched in cell cycle and apoptosis-related pathways, and (3) whether a virus could be enriched in protein metabolism-related pathways. *R* package ClusterProfiler for biological term classification and enrichment analysis of proteins was used.

Enrichment analyses in optimization of druggable VTHPs

Enrichment analyses of EGEPs, membrane and hub proteins were conducted by hypergeometric test using 'phyper' and 'fisher.test' functions in *R* package stats. A *P*-value of <0.05 indicates a significant difference between druggable essential, membrane, hub VTHPs and other proteins.

Construction of drug-virus network (DVN)

The shared candidate VTHPs were the basis of connections between viruses and known drugs. A connection was established between a drug and a virus if at least one of the drug targets has been proved to be VTHP(s) of the virus (Website Table 4). The DVN was visualized and illustrated using the Cytoscape software (Figure 3A).

Simulation and evaluation of synergy effect

Synergy effects of combinations of predicted and clinically used drugs were measured using the *R* package SynergyFinder based on the Loewe additivity model, which has been proved to be an easy and flexible approach in drug combination studies [59]. If the combined effect is greater than addition of the expected effect of each drug, the response is synergy (synergy score > 0) whereas antagonism is concluded when the combination produces less than expected effect (synergy score < 0).

Antiviral activity tests against HHV-1

HHV-1 SM44 strain was obtained from the Beijing Institute of Biological Products Co., Ltd. Vero cells were purchased from National Collection of Authenticated Cell Cultures (NCACC, GNO10, passage 93), China. The cells were cultured in Dulbecco's modified Eagle's medium (DMEM, Invitrogen) supplemented with 10% (vol/vol) fetal bovine serum (Gibco), 2 mM glutamine, 100 unit/ml penicillin and 100 μg/ml streptomycin at 37°C in 5% CO_2.

Vero cells were inoculated in 96-well plates, cultured to semiconfluence and infected with HHV-1 (100 $TCID_{50}$). We removed the HHV-1 solution after 2 h and replaced it with serial dilutions of the predicted and control compounds. The plates were incubated at 37°C for 3 days. Antiviral activity (IC_{50}) was used to evaluate the effect of tested drugs using CPE reduction on D3. It was observed using a Leica EL6000 microscope (Leica Microsystems, Germany) [60].

Cytotoxicity (TC_{50}) of the compounds was determined by MTT assay. Monolayer cells were washed twice with

serum-free DMEM. The culture medium containing different concentrations of the tested drugs was added, and the cells were incubated at 37°C in 5% CO_2 for 48 h. Cell viability was observed and expressed as optical density [61, 62]. Absorbance was read at 570 nm by spectrophotometry using a microplate reader (BioTeK Instruments, USA). MTT cell proliferation and cytotoxicity assay kit (C0009M, Beyotime, Shanghai, China) was used.

A treatment index (TI) value was defined as the ratio of TC_{50}/IC_{50}. At least three independent experiments were conducted.

Antiviral activity tests against HBV

The HBV-expressing stable cell line HepG2.2.15 (passage 32) [63] was provided by Yumei Wen, Fudan University, China and cultured in the same condition as Vero cells.

The cells were treated with the tested drugs at serial dilutions, and the culture medium was changed every 3 days. On D3, D6 and D9, the culture supernatants were collected for analyses of viral proteins (HBsAg and HBeAg) and HBV-DNA. The viral proteins were detected using ELISA kits (Shanghai Kehua Bio-engineering Co., Ltd., Shanghai, China). HBV-DNA in culture supernatants was detected by quantitative PCR (qPCR) (Table S4 available online at http://bib.oxfordjournals.org/). The qPCR analysis was performed using SYBR Premix Ex Taq™ (TaKaRa) and the StepOne Plus real-time PCR system (Thermo Fisher Scientific) and the thermocycling parameters were set as follows: maintained at 95°C for 5 min, followed by 40 cycles of 95°C for 15 s and 60°C for 1 min. TC_{50} of tested drugs was determined by MTT assay. At least three biological and technical replicates were performed to allow accurate quantification by statistical analyses.

Antiviral activity tests against IAV

For *in vitro* tests, IAV H1N1 A/PR/8/34 (VR-95) and H3N2 A/Hong Kong/8/68 (VR-1679) from American type culture collection (ATCC) were used. MDCK cells (NCACC, GNO23, passage 27) were maintained in the same condition as Vero cells. They were infected with 10 $TCID_{50}$ of the virus strain for 2 h and treated with the tested drugs at serial dilutions. IC_{50} and TC_{50} were evaluated by CPE reduction and MTT assay, respectively. Each measurement was performed in triplicate.

For *in vivo* tests, the highly virulent and mouse-adapted IAV H1N1 A/FM/1/47 (VR-97, ATCC) was used. It was supplied by Shanghai Center for Disease Control and Prevention (Shanghai, China) and stored in aliquots at −70°C. Male BALB/c mice (16–18 g, 6–8 weeks) from the Shanghai SLACCAS Laboratory Animal Co., Ltd. (Shanghai, China) were housed under a specific pathogen-free (SPF) condition, and sterile water and standard mouse chow were provided. All experimental protocols were approved by the Animal Experiment Committee in Fudan University (Shanghai, China).

Mice were randomly divided into nine groups: normal control group, virus control group, oseltamivir group (15 mg/kg), dextromethorphan groups (15, 30, 60 mg/kg) and dextromethorphan + oseltamivir groups (15 mg/kg + 15 mg/kg, 30 mg/kg + 15 mg/kg, 60 mg/kg + 15 mg/kg). All mice except the control were anesthetized under 1% pentobarbital and infected intranasally (i.n.) with 10 LD_{50} (equal to 2.1×10^3 PFU) of IAV H1N1 in 30 μl inoculum volume per mouse. Mice were treated with different doses of dextromethorphan, oseltamivir or their combinations by gavage once daily for 5 days 48 h after infection. The mice were monitored for survival and body weight loss for 11 days. On the 12th day, all mice were sacrificed and lungs were collected and weighed. Lung injury score was evaluated by hyperemic and parenchymal lesion, and lung index was calculated as the ratio of average lung weight to average body weight to indicate edema and inflammation of lungs. Protein concentration was determined by BCA assay (P0010, Beyotime, Shanghai, China).

Statistical analyses

All statistical analyses were performed using GraphPad Prism for Windows (Version 6.0) and expressed as mean ± SD. Survival of mice was analyzed by the Gehan–Breslow–Wilcoxon test. Other experimental data were evaluated by a two-tailed Student's *t*-test or one-way ANOVA followed by Bonferroni's test. In all cases, probability levels less than 0.05 ($P < 0.05$) were considered to indicate statistical significance.

Key Points

- We performed a comprehensive investigation of VTHPs and proposed a new classification of viral infections based on enriched signaling pathways of VTHPs.
- We have optimized druggable VTHPs and concluded that nonessential membrane and hub proteins are potential ideal targets for development of host-directed repositioned antiviral therapeutics.
- We constructed DVN and analyzed antiviral repositioning potential of approved drugs. The *in vitro* and *in vivo* tests confirmed the predicted bosutinib against HHV-1, maraviroc against HBV and dextromethorphan against IAV.
- Our work revealed new rules in viruses, VTHPs and known drugs, and proposed promising candidate targets and compounds for further clinical studies, providing an innovative and powerful approach for drug discovery based on host-directed repositioning strategy.

Supplementary data

Supplementary data are available online at https://academic.oup.com/bib.

Funding

National Natural Science Foundation of China (62103436, 81803431).

References

1. Navratil V, de Chassey B, Meyniel L, *et al.* VirHostNet: a knowledge base for the management and the analysis of proteome-wide virus-host interaction networks. *Nucleic Acids Res* 2009;**37**:D661–8.
2. Cohen ML. Changing patterns of infectious disease. *Nature* 2000;**406**:762–7.
3. Clercq ED. Antivirals and antiviral strategies. *Nat Rev Microbiol* 2004;**2**:704–20.
4. Tan SL, Ganji G, Paeper B, *et al.* Systems biology and the host response to viral infection. *Nat Biotechnol* 2007;**25**:1383–9.
5. Chiara M, D'Erchia AM, Gissi C, *et al.* Next generation sequencing of SARS-CoV-2 genomes: challenges, applications and opportunities. *Brief Bioinform* 2021;**22**:616–30.
6. De Clercq E, Li G. Approved antiviral drugs over the past 50 years. *Clin Microbiol Rev* 2016;**29**:695–747.
7. Guirimand T, Delmotte S, Navratil V. VirHostNet 2.0: surfing on the web of virus/host molecular interactions data. *Nucleic Acids Res* 2015;**43**:D583–7.
8. Calderone A, Licata L, Cesareni G. VirusMentha: a new resource for virus-host protein interactions. *Nucleic Acids Res* 2015;**43**:D588–92.
9. Kinnings SL, Liu N, Buchmeier N, *et al.* Drug discovery using chemical systems biology: repositioning the safe medicine Comtan to treat multi-drug and extensively drug resistant tuberculosis. *PLoS Comput Biol* 2009;**5**:e1000423.
10. Doerig C, Meijer L. Antimalarial drug discovery: targeting protein kinases. *Expert Opin Ther Targets* 2007;**11**:279–90.
11. Zhou X, Dai E, Song Q, *et al.* In silico drug repositioning based on drug-miRNA associations. *Brief Bioinform* 2020;**21**:498–510.
12. Kellam P. Attacking pathogens through their hosts. *Genome Biol* 2006;**7**:201.
13. Xue H, Li J, Xie H, *et al.* Review of drug repositioning approaches and resources. *Int J Biol Sci* 2018;**14**:1232–44.
14. Parvathaneni V, Kulkarni NS, Muth A, *et al.* Drug repurposing: a promising tool to accelerate the drug discovery process. *Drug Discov Today* 2019;**24**:2076–85.
15. Wu C-K, Zhang X-C, Yang Z-J, *et al.* Learning to SMILES: BAN-based strategies to improve latent representation learning from molecules. *Brief Bioinform* 2021;**22**:bbab327.
16. Zhang X-C, Wu C-K, Yang Z-J, *et al.* MG-BERT: leveraging unsupervised atomic representation learning for molecular property prediction. *Brief Bioinform* 2021;**22**:bbab152.
17. Xiong G, Wu Z, Yi J, *et al.* ADMETlab 2.0: an integrated online platform for accurate and comprehensive predictions of ADMET properties. *Nucleic Acids Res* 2021;**49**:W5–14.
18. Yang X, Wang W, Ma J-L, *et al.* BioNet: a large-scale and heterogeneous biological network model for interaction prediction with graph convolution. *Brief Bioinform* 2022;**23**:bbab491.
19. Li Z, Zhong Q, Yang J, *et al.* DeepKG: an end-to-end deep learning-based workflow for biomedical knowledge graph extraction, optimization and applications. *Bioinforma Oxf Engl* 2021;**38**:1477–1479.
20. Wang W, Yang X, Wu C, *et al.* CGINet: graph convolutional network-based model for identifying chemical-gene interaction in an integrated multi-relational graph. *BMC Bioinformatics* 2020;**21**:544.
21. Reeves PM, Bommarius B, Lebeis S, *et al.* Disabling poxvirus pathogenesis by inhibition of Abl-family tyrosine kinases. *Nat Med* 2005;**11**:731–9.
22. Ito T, Itakura J, Takahashi S, *et al.* Sprouty-related Ena/vasodilator-stimulated phosphoprotein homology 1-domain-containing Protein-2 critically regulates influenza a virus-induced pneumonia. *Crit Care Med* 2016;**44**:e530–43.
23. Bordier BB, Marion PL, Ohashi K, *et al.* A Prenylation inhibitor prevents production of infectious Hepatitis Delta virus particles. *J Virol* 2002;**76**:10465–72.
24. Clouser CL, Patterson SE, Mansky LM. Exploiting drug repositioning for discovery of a novel HIV combination therapy. *J Virol* 2010;**84**:9301–9.
25. Li R, Li Y, Liang X, *et al.* Network pharmacology and bioinformatics analyses identify intersection genes of niacin and COVID-19 as potential therapeutic targets. *Brief Bioinform* 2021;**22**:1279–90.
26. Han Y, Wang Z, Ren J, *et al.* Potential inhibitors for the novel coronavirus (SARS-CoV-2). *Brief Bioinform* 2021;**22**:1225–31.
27. Gao J, Tian Z, Yang X. Breakthrough: chloroquine phosphate has shown apparent efficacy in treatment of COVID-19 associated pneumonia in clinical studies. *Biosci Trends* 2020;**14**:72–3.
28. Khalili JS, Zhu H, Mak NSA, *et al.* Novel coronavirus treatment with ribavirin: groundwork for an evaluation concerning COVID-19. *J Med Virol* 2020;**92**:740–6.
29. McKee DL, Sternberg A, Stange U, *et al.* Candidate drugs against SARS-CoV-2 and COVID-19. *Pharmacol Res* 2020;**157**:104859.
30. Bouhaddou M, Memon D, Meyer B, *et al.* The global phosphorylation landscape of SARS-CoV-2 infection. *Cell* 2020;**182**:685–712.e19.
31. Wang Y-C, Chen S-L, Deng N-Y, *et al.* Network predicting drug's anatomical therapeutic chemical code. *Bioinformatics* 2013;**29**:1317–24.
32. Morgnanesi D, Heinrichs EJ, Mele AR, *et al.* A computational chemistry perspective on the current status and future direction of hepatitis B antiviral drug discovery. *Antiviral Res* 2015;**123**:204–15.
33. Wang T, Birsoy K, Hughes NW, *et al.* Identification and characterization of essential genes in the human genome. *Science* 2015;**350**:1096–101.
34. Bartha I, di Iulio J, Venter JC, *et al.* Human gene essentiality. *Nat Rev Genet* 2018;**19**:51–62.
35. Begum T, Ghosh TC, Basak S. Systematic analyses and prediction of human drug side effect associated proteins from the perspective of protein evolution. *Genome Biol Evol* 2017;**9**:337–50.
36. Iwasaki M, Minder P, Caì Y, *et al.* Interactome analysis of the lymphocytic choriomeningitis virus nucleoprotein in infected cells reveals ATPase Na^+/K^+ transporting subunit alpha 1 and prohibitin as host-cell factors involved in the life cycle of mammarenaviruses. *PLoS Pathog* 2018;**14**:e1006892.
37. Lapošová K, Pastoreková S, Tomášková J. Lymphocytic choriomeningitis virus: invisible but not innocent. *Acta Virol* 2013;**57**:160–70.
38. Zawilińska B, Kosz-Vnenchak M. General introduction into the Ebola virus biology and disease. *Folia Med Cracov* 2014;**54**:57–65.
39. Baseler L, Chertow DS, Johnson KM, *et al.* The pathogenesis of Ebola virus disease. *Annu Rev Pathol* 2017;**12**:387–418.
40. Hickson SE, Margineantu D, Hockenbery DM, *et al.* Inhibition of vaccinia virus replication by nitazoxanide. *Virology* 2018;**518**:398–405.
41. Smith GL. Vaccinia virus protein C6: a multifunctional interferon antagonist. *Adv Exp Med Biol* 2018;**1052**:1–7.
42. Gaspar M, May JS, Sukla S, *et al.* Murid herpesvirus-4 exploits dendritic cells to infect B cells. *PLoS Pathog* 2011;**7**:e1002346.
43. Rucevic M, Hixson D, Josic D. Mammalian plasma membrane proteins as potential biomarkers and drug targets. *Electrophoresis* 2011;**32**:1549–64.
44. Lúcio M, Lima JLFC, Reis S. Drug-membrane interactions: significance for medicinal chemistry. *Curr Med Chem* 2010;**17**:1795–809.

45. Kumar N, Sharma S, Kumar R, *et al.* Host-directed antiviral therapy. *Clin Microbiol Rev* 2020;**33**:e00168–19.
46. Han J, Perez JT, Chen C, *et al.* Genome-wide CRISPR/Cas9 screen identifies host factors essential for influenza virus replication. *Cell Rep* 2018;**23**:596–607.
47. Boguski MS, Mandl KD, Sukhatme VP. Drug discovery. Repurposing with a difference. *Science* 2009;**324**:1394–5.
48. Rasheed S, Sánchez SS, Yousuf S, *et al.* Drug repurposing: in-vitro anti-glycation properties of 18 common drugs. *PLoS One* 2018;**13**:e0190509.
49. DeFilippis V, Früh K. Host cell targets for antiviral therapy: an update. *Future Virol* 2006;**1**:509–18.
50. Kaufmann SHE, Dorhoi A, Hotchkiss RS, *et al.* Host-directed therapies for bacterial and viral infections. *Nat Rev Drug Discov* 2018;**17**:35–56.
51. Echeverría-Esnal D, Martin-Ontiyuelo C, Navarrete-Rouco ME, *et al.* Azithromycin in the treatment of COVID-19: a review. *Expert Rev Anti Infect Ther* 2021;**19**:147–63.
52. Majumder J, Minko T. Recent developments on therapeutic and diagnostic approaches for COVID-19. *AAPS J* 2021;**23**:14.
53. Akbarzadeh-Khiavi M, Torabi M, Rahbarnia L, *et al.* Baricitinib combination therapy: a narrative review of repurposed Janus kinase inhibitor against severe SARS-CoV-2 infection. *Infection* 2021;**13**:1–14.
54. Xiong G, Yang Z, Yi J, *et al.* DDInter: an online drug-drug interaction database towards improving clinical decision-making and patient safety. *Nucleic Acids Res* 2022;**50**:D1200–7.
55. Yang X, Wu C, Nenadic G, *et al.* Mining a stroke knowledge graph from literature. *BMC Bioinformatics* 2021;**22**:387.
56. Wu C, Xiao X, Yang C, *et al.* Mining microbe-disease interactions from literature via a transfer learning model. *BMC Bioinformatics* 2021;**22**:432.
57. Xing Y, Wu C, Yang X, *et al.* ParaBTM: a parallel processing framework for biomedical text mining on supercomputers. *Mol Basel Switz* 2018;**23**:E1028.
58. Jiang Y, Wu C, Zhang Y, *et al.* Digest.VCF: an online NGS data interpretation system based on intelligent gene ranking and large-scale text mining. BMC med. *Genomics* 2019;**12**:193.
59. He L, Kulesskiy E, Saarela J, *et al.* Methods for high-throughput drug combination screening and synergy scoring. *Methods Mol Biol Clifton NJ* 2018;**1711**:351–98.
60. Clements ML, Betts RF, Murphy BR. Advantage of live attenuated cold-adapted influenza a virus over inactivated vaccine for a/Washington/80 (H3N2) wild-type virus infection. *Lancet Lond Engl* 1984;**1**:705–8.
61. Kumar P, Nagarajan A, Uchil PD. Analysis of cell viability by the MTT assay. *Cold Spring Harb Protoc* 2018;**2018**:469–472.
62. Pozzolini M, Scarfi S, Benatti U, *et al.* Interference in MTT cell viability assay in activated macrophage cell line. *Anal Biochem* 2003;**313**:338–41.
63. Sells MA, Chen ML, Acs G. Production of hepatitis B virus particles in hep G2 cells transfected with cloned hepatitis B virus DNA. *Proc Natl Acad Sci U S A* 1987;**84**:1005–9.